Microsolvation of Li^+ in Water Analyzed by Ionization and Double Ionization

Imke B. Müller* and Lorenz S. Cederbaum

Theoretische Chemie, Physikalisch-Chemisches Institut, Universität Heidelberg, Im Neuenheimer Feld 229, D-69120 Heidelberg, Germany

Francesco Tarantelli

Dipartimento di Chimica and CNR I.S.T.M., Università di Perugia, I-06123 Perugia, Italy

Received: February 17, 2004; In Final Form: April 20, 2004

The microsolvation of Li^+ in water is investigated. The ionization and double-ionization spectra of the series of $(H_2O)_nLi^+$ ($n = 1-5$) clusters are calculated ab initio by Green's function methods and discussed in detail. The impact of the solvation of the lithium cation with an increasing number of water molecules on the spectral characteristics is revealed. In the context of microsolvation, the discussion of the results for the $(H_2O)_5Li^+$ cluster is particularly important because the second solvation shell is accessed. Ionization- and double-ionization spectra may be considered to be very useful for the study of microsolvation clusters.

I. Introduction

Cluster systems attract considerable research interest because they are considered to be the intermediate stage between isolated molecules in the gas phase and molecules in solution or bulk media. Clusters consisting of solvent molecules and one heteromolecule, in particular, serve as model systems to elucidate the first steps of the solvation process.[1,2] Because water is the predominant solvent in nature, solvation by water is addressed by many theoretical and experimental studies. Concerning the solvation of inorganic cations and anions, one of the topics at the focus of many Monte Carlo molecular dynamics simulations[3−9] as well as of ab initio studies[10−12] and experiments[1] is the determination of the coordination number of the ion in the first solvation shell.

An experimental method that is applied to determine the structural characteristics of clusters, often aided by ab initio structure optimization, is a combination of photoelectron spectroscopy and mass spectrometry. Usually, photoionization is used to prepare the cluster of interest, and subsequently, time-of-flight mass spectrometry is applied to analyze and characterize its structural properties. However, a few examples where photoelectron spectroscopy is used to characterize the clusters prepared experimentally by other means are reported in the literature. Some examples of the interplay of photoelectron spectroscopy and ab initio calculations are a study of $Li_n(OH)_{n-1}$ clusters by Tanaka et al.[13,14] and earlier studies by Schultz et al.[15]

The evolution of photoelectron spectroscopy to tunable synchrotron sources increases the energy range that is accessible to the investigation of electronic properties.[16] It is possible to ionize inner valence electrons by means of modern radiation sources, whereas only outer valence electrons could be ionized by the commonly used He(I) sources.[17] This progress in experimental techniques has also led to increasing interest in theoretical studies of inner valence ionization spectra because they are very complex because of the phenomenon of the breakdown of the orbital picture of ionization.[18] For cluster systems in particular, the increasing interest in inner valence ionization spectra has resulted in the prediction of new electronic relaxation mechanisms following inner valence ionization of neutral clusters, which is not possible for their constituent monomers.[19] A cluster-specific intermolecular electronic decay mechanism following inner valence ionization, the intermolecular coulombic decay (ICD) mechanism, has been predicted, for example, for $(HF)_n$, $n = 2-4$ clusters[19,20] and also for the microsolvated HF in $(H_2O)_2HF$.[21] Other systems of interest were atomic clusters, for example, $(Ne)_n$, with n ranging up to 13.[22,23] A related decay mechanism, electron-transfer-mediated electronic decay (ETMD), has been described for heteroclusters such as NeAr.[24] ICD has been recently experimentally confirmed by the detection of the secondary electron emitted upon inner valence ionization of large $(Ne)_n$ clusters.[25]

In this paper, we study the influence of the number of solvation water molecules coordinated by cations on their ionization- and double-ionization spectra. Our method of choice for the calculation of these spectra is the Green's functions approach,[26−30] utilizing the ADC(3) method[31−33] for the ionization and the ADC(2) method[34,35] for the double-ionization spectra. Aiming at the analysis of the complete valence ionization of the clusters under investigation, we have to apply a theoretical method that takes many-body effects into account. Green's function methods in general and the ADC approach in particular have proven to be very useful for the calculation of ionization- and double-ionization spectra in many applications, (e.g., refs 36−42).

In this contribution, we chose to study the cations $(H_2O)_n$-Li^+ to derive the influence of solvation on the ionization properties of positively charged solvation clusters in general. Lithium solvation in water has attracted and is still attracting a lot of interest in the literature because the cations are rather ubiquitous in nature and involved in several interesting processes. By analyzing the ionization- and double-ionization spectra of cluster systems modeling the solvation of lithium cations, we expect to provide helpful information, in particular, for experiments on solvation using photoelectron spectroscopy.

* Corresponding author. E-mail: imke.mueller@tc.pci.uni-heidelberg.de.

10.1021/jp0492826 CCC: $27.50
Published on Web 06/15/2004

II. Methods and Computational Details

All ionization- and double-ionization spectra discussed in this contribution have been calculated by Green's function methods. Green's function methods allow for a direct computation of ionization energies by searching for the poles of the appropriate Green function. The corresponding pole strengths are related to spectral intensities. These poles and pole strengths are obtained by solving an eigenvalue equation.[31] Green's function methods possess several advantageous properties. Among others, they provide the spectra directly and are size-consistent. The latter is a particularly important property when dealing with a series of cluster systems.

The one-particle Green function is evaluated according to a third-order algebraic diagrammatic construction scheme [ADC-(3)]. The ADC scheme transforms the problem of determining the poles and the corresponding pole strengths of the Green function to a matrix eigenvalue problem utilizing a diagrammatic perturbation theory based on a Hartree−Fock (HF) ground-state ansatz. Details about the ADC(3) scheme may be found elsewhere.[31−33]

We adopt the following nomenclature here: configurations derived from the HF ground state by removing one electron from an occupied orbital are referred to as 1h configurations (one-hole configuration). Configurations derived from adding one electron to an occupied orbital of a HF ground state are referred to as 1p configurations (one-particle configuration). 2h1p configurations are derived from a HF ground state by adding one electron to an unoccupied orbital and removing two electrons from occupied orbitals. 2p1h configurations are formed analogously by adding two electrons to unoccupied orbitals of the HF ground state and removing one electron from an occupied orbital.

Owing to the Dyson equation[26] behind the ADC(3) approach applied here, the ADC(3) matrix includes not only the large ionization block spanned by the 2h1p configurations but also an even larger affinity block because all 2p1h configurations have to be taken into account. These two blocks, in particular, the affinity block, are the leading contributions to the matrix dimension. The ionization and affinity blocks are not directly coupled in the ADC matrix, but they are indirectly coupled. The coupling of the large blocks is achieved via their respective direct coupling to the comparatively small 1h+1p configuration block. It is therefore not possible to neglect the affinity block completely without causing shifts in the ionization energies. However, because the ionization block and the 1h1p block comprise the predominant contributions to the ionization energies, it is justified to replace the affinity block with a reduced affinity block of small dimension preserving the information of the correct spectral envelope. This reduction is done by a few (in this contribution 10) iterations of the Block−Lanczos algorithm[33,35,43] to the affinity block.

The reduction of the affinity block leads to a substantial reduction of the matrix dimension that makes a full diagonalization of the ADC(3) matrixes build up for the clusters $(H_2O)_n$-Li^+, $n = 1-4$, feasible. The reduced matrix dimensions for the $n = 3$ or 4 clusters are in the range of 12 000 for the basis sets used here. The reduced ADC matrix set up for the $(H_2O)_5Li^+$ cluster, which is in the range of 36 000, was diagonalized by Block−Lanczos iterations until the ionization spectrum was converged.

To characterize the ionized states, we apply a 1h population analysis.[21] The 1h population analysis assigns the ionized states to the contributing atoms or cluster fragments. This information is mapped in the 1h contribution(s) of each ionized state.

Double-ionization spectra are provided by poles and pole strengths of the particle−particle propagator. The particle−particle propagator is evaluated according to a second-order algebraic diagrammatic construction scheme [ADC(2)] based on the HF ground state. Because there is no analogue to the Dyson equation for the particle−particle propagator, the ADC-(2) matrix does not contain an affinity part. Nevertheless, the ADC(2) matrix for the particle−particle propagator is a high-dimensional matrix because all 3h1p configurations have to be taken into account. We performed direct ADC(2) calculations, which means that the large ADC(2) matrix is never explicitly built up and stored on the hard disk.[44] Matrix element blocks are calculated from suitably sorted two-electron integrals and orbital energies when they are needed for the matrix × vector multiplication during the Block−Lanczos procedure and are directly passed to the Lanczos diagonalizer. The Block−Lanczos algorithm implemented allows for the calculation of approximate eigenvectors. The convergence, according to a residue criterion, of the relevant part of the double-ionization spectra was achieved after 400 block iterations, the number of start vectors depending on the dimensions of the 2h block. The states comprising the double-ionization spectra are characterized using a 2h population analysis,[45] which indicates the localization of the two holes on the cluster monomers.

All Green's function calculations have been performed at the optimized ab initio equilibrium geometries discussed in the next section. The optimized structures and the Hartree−Fock orbital bases for the ADC calculations were computed using the GAMESS-UK program package.[46] The Green's function calculations are performed using an ADC program package described in refs 33, 35, and 45 and references therein. For all calculations presented here, we used the correlation-consistent Dunning basis set of double-ζ quality (cc-pVDZ),[47,48] including polarization functions. All basis sets were taken from a basis set library.[49] The basis set is augmented by one set of diffuse (s, p, d) functions on each oxygen atom for all cluster systems (aug-cc-pVDZ).[50,51] One set of diffuse functions is added to each hydrogen atom except for the clusters containing four and five water molecules. Corresponding basis sets have been reported to give reasonable results describing ground-state properties and geometries of $Li^+(H_2O)_n$, $n = 1-6$ clusters.[10] It has been shown that diffuse functions, which we use on oxygen for all calculations and on hydrogen for all but the largest clusters ($n = 4$ or 5), are extremely important for a correct cluster description because they decrease the basis set superposition error significantly.[10,52] The aug-cc-pVDZ basis set chosen here seems to provide a good compromise between the feasibility of the calculations and the accuracy of the results. In all calculations, the O(1s) orbitals as well as their highest-lying virtual counterparts have been excluded from the active configuration space. The exclusion of these orbitals from the active space is justified by the large energy gap between the core orbitals and the valence orbitals.

III. Cluster Geometries

The geometries of $Li^+(H_2O)_n$ clusters, $n = 1-6$, have been optimized in ref 10 by Feller et al. using basis sets from the (aug)-cc-pVXZ family at the restricted HF and MP2 (second-order Moller−Plesset perturbation theory) levels. Because the data for $(H_2O)_5Li^+$ is incomplete in ref 10, we decided to reoptimize the cluster geometries on the MP2 level using our chosen basis sets. The optimizations were constrained within the respective ground-state symmetry of each cluster found in ref 10. The resulting structures, which are depicted in Table 1,

TABLE 1: Symmetry-Restricted MP2 Optimized Geometries of the Four Water−Lithium Clusters Discussed[a]

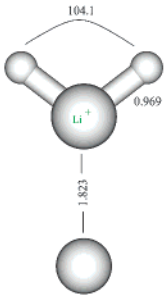

$H_2O\ Li^+$

C_{2v}

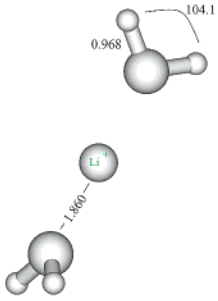

$(H_2O)_2\ Li^+$

D_{2d}

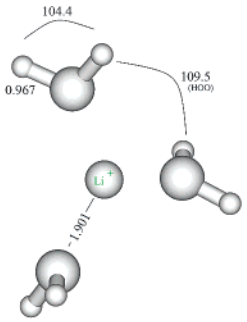

$(H_2O)_3\ Li^+$

D_3

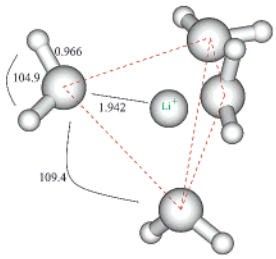

$(H_2O)_4\ Li^+$

S_4

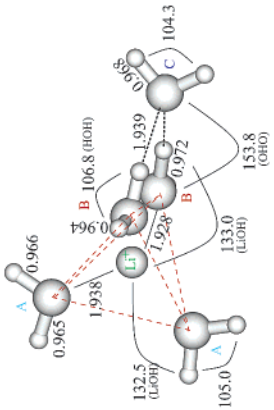

$(H_2O)_5\ Li^+$

C_2

[a] All bond lengths are given in angstroms, and all angles are given in degrees.

TABLE 2: Hartree−Fock and MP2 Energies of All $(H_2O)_nLi^+$ Clusters Treated

cluster	energy HF (hartrees)	energy MP2 (hartrees)	cluster	energy HF (hartrees)	energy MP2 (hartrees)
H_2O	−76.041	−76.270	$(H_2O)_3Li^+$	−235.500	−236.191
$H_2O\ Li^+$	−83.333	−83.563	$(H_2O)_4\ Li^+$	−311.565	−312.479
$(H_2O)_2\ Li^+$	−159.423	−159.885	$(H_2O)_5\ Li^+$	−387.625	−388.772

are not very different from, though not identical to, the ground-state geometries reported in ref 10. In particular, the Li−O distance is systematically slightly shorter in our results. Table 2 shows the computed total energies of the optimized structures. As one can see, each cluster is stable toward dissociation into the next smallest cluster and a water molecule.

For $n = 1-4$, the number of water molecules in the cluster is not larger than the number of water molecules that usually comprise the first solvation shell of the lithium cation. Consequently, the geometries of the clusters are determined first by the tendency of all water molecules to bind to the lithium cation through the oxygen and second by the tendency to minimize the steric hindrance between hydrogen atoms without disturbing the typical water HOH angle too much. The resulting structures are highly symmetric. H_2OLi^+ is C_{2v}-symmetric with two equivalent hydrogen atoms. D_{2d} symmetry with two equivalent water molecules, which are situated on perpendicular planes, is found for $(H_2O)_2Li^+$. As in ref 10, $(H_2O)_3Li^+$ has been optimized in D_3 symmetry, whereas the $(H_2O)_4Li^+$ cluster was optimized in D_2 symmetry, very close to the S_4 symmetry reported in ref 10. All water units are equivalent (approximately equivalent for $n = 4$) by symmetry for these clusters.

The $(H_2O)_5Li^+$ cluster is the only cluster that we studied where the number of water ligands exceeds that which may be directly bound to a lithium cation. The fifth water molecule is thus hydrogen bonded to two water units of the first solvation shell. This distorts the $(H_2O)_4Li^+$-like structure of the other four water molecules into a C_2-symmetric structure.

The relatively high symmetry of the $(H_2O)_nLi^+$ clusters enables us to apply large basis sets without increasing the computational demand beyond feasibility. This point is important for our purposes because large basis sets have to be used to achieve reliable results in the simulation of inner valence ionization spectra.

IV. Ionization Characteristics of $(H_2O)_nLi^+$, $n = 1-4$ Clusters

A. Comparison of the Spectra of H_2OLi^+ to Those of Water and Li^+. The ionization spectrum of H_2OLi^+ can be divided into a spectrum related to the water molecule and a spectrum related to the lithium ion in the cluster. As can be

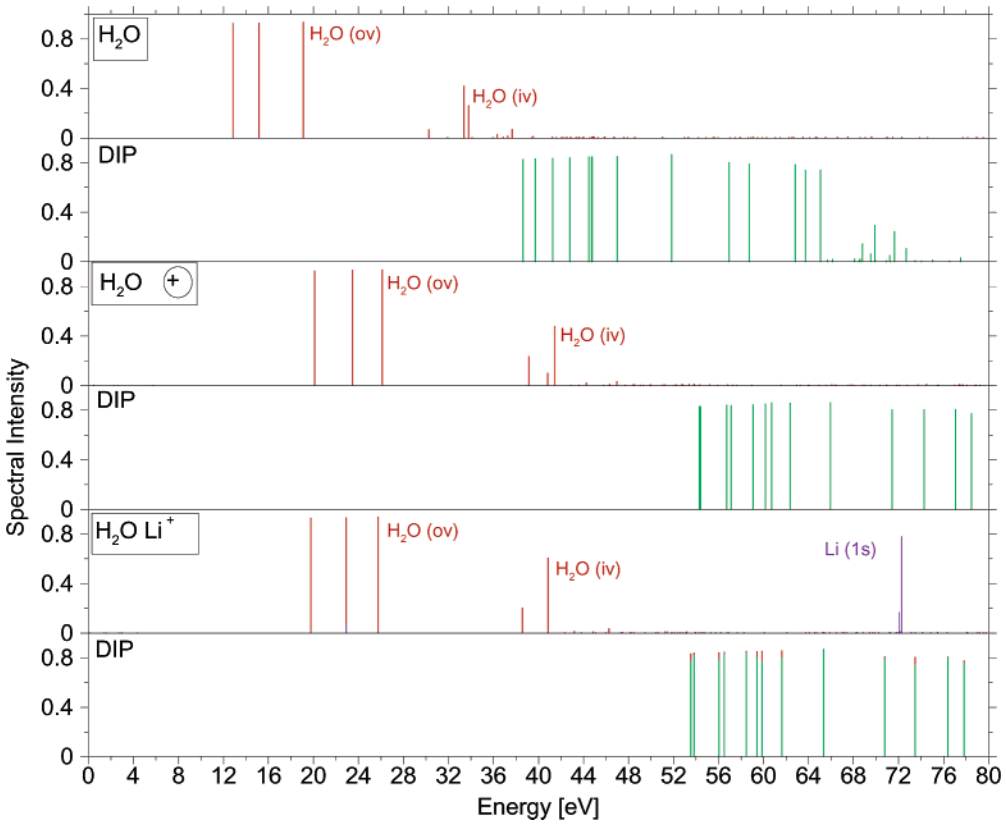

Figure 1. Ionization and double-ionization spectra (indicated by DIP) of H_2O, $H_2O\oplus$, and H_2OLi^+. The symbol $\oplus$ indicates a point charge added to H_2O at the position of the Li^+ in H_2OLi^+. Note the similarity of those parts of the spectra of H_2OLi^+ and $H_2O\oplus$ corresponding to water. iv stands for inner valence, and ov, for outer valence electrons. Coloring of ionization spectra: red, 1h contribution on water; violet, 1h contribution on lithium. Coloring of double-ionization spectra: green, 2h contribution localized on one water molecule (one site states); black, 2h contribution delocalized over two water molecules (two site states); and red, 2h contribution describing one hole on water and one on lithium.

seen in Figure 1, these two subspectra are also well separated energetically. Most of the water spectrum is below 50 eV, and lithium ionization is found above 70 eV. The water ionization subspectrum of the H_2OLi^+ cluster is shifted by about 7 eV toward higher ionization energies compared to that of a free water molecule. The overall pattern of lines in the H_2OLi^+ spectrum resembles, however, that of the free-water spectrum. (Finer differences will be discussed shortly.) The 7-eV shift in the spectrum is a consequence of the positive net charge of the H_2OLi^+ cluster. The initial positive net charge of the cluster and the hole charge created by ionization repel each other such that the ionization of positively charged clusters requires more energy than for neutral clusters. Indeed, the electrostatic repulsion of two naked charges localized on the Li and O atoms amounts to 7.9 eV. To determine the impact of the positive charge on the ionization- and double-ionization spectra, we also computed the corresponding spectra of the water molecule in the field of a positive point charge. The point charge has been placed at the site that the Li atom occupies in the H_2OLi^+ cluster. The spectra of free water and water in the field of the positive point charge, denoted $H_2O\oplus$ and H_2OLi^+, are compared in Figure 1. It is obvious from the similarity of the water subspectra of $H_2O\oplus$ and H_2OLi^+ that the energy shift with respect to the neutral free water and other details as well are totally explained by the mere presence of the positive charge introduced by the lithium cation.

Let us now pay attention to the fine structure of the spectra. Apart from the overall 7-eV shift, there are some differences between the ionization spectrum of H_2OLi^+ and that of free water. The second line in the low-energy spectrum of the cluster is subject to a slightly larger energy shift toward higher energies than the other two lines in the outer valence spectrum. To explain this, we note that this line describes the ionization of the water outer valence orbital of a_1 symmetry and this orbital interacts more effectively with the charge on Li than the other two outer valence orbitals of water of b_2 and b_1 symmetry because it points directly to the lithium cation. In fact, we see that the relative shift of the corresponding spectral line compared to the free-water line is even slightly more pronounced in the case of $H_2O\oplus$, where this interaction is less screened.

More significant differences between the ionization spectra of free water and H_2OLi^+ are found in the inner valence part of the spectra. The breakdown of the molecular orbital picture is more pronounced in the spectrum of free water than in that of H_2OLi^+. To explain the smaller number of ionic states carrying intensity in the spectrum of H_2OLi^+, we may note that the stabilization of the water electrons in the cluster has the consequence that excited configurations of 2h1p character are generally shifted to higher energy, relative to that of the 1h configurations, than in the case of free water. The interaction of the inner valence 1h configuration with 2h1p configurations is thus weaker for H_2OLi^+ than for the water molecule, and this leads to a less-pronounced line breakdown. The above explanation is supported by the result that the inner valence spectrum of $H_2O\oplus$ is in accord with that of H_2OLi^+.

We briefly address the impact of the positive charge on the first double-ionization potential here; the double ionization spectrum is discussed in detail in section V. The first double-ionization potentials (DIP) of neutral free water and H_2OLi^+ differ by the large amount of 15 eV. The difference in the potentials is totally explained by the mere presence of the positive charge on the lithium cation. The electrostatic interac-

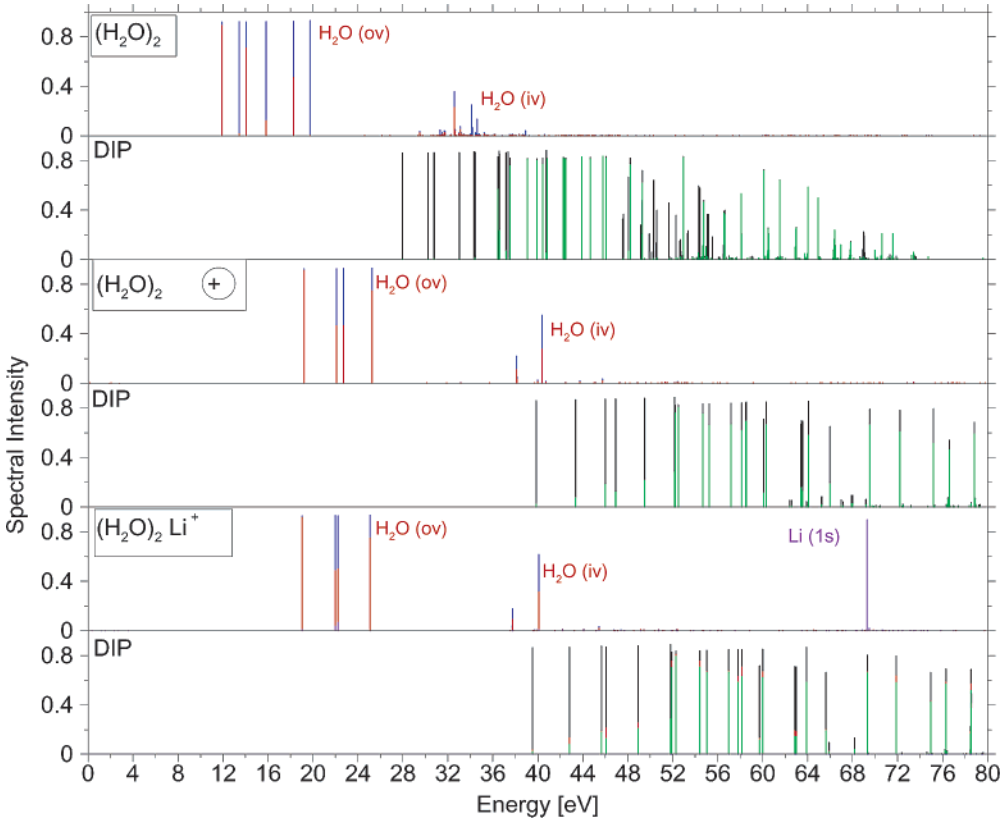

Figure 2. Ionization and double-ionization spectra of $(H_2O)_2$, $(H_2O)_2\oplus$, and $(H_2O)_2Li^+$. The symbol $\oplus$ indicates a point charge at the site that the lithium cation occupies in the $(H_2O)_2Li^+$ cluster. Coloring of the ionization spectra: red, 1h contribution on one water; blue, 1h contribution on the other one; violet, 1h contribution on lithium. Coloring of double-ionization spectra: green, 2h contribution localized on one water molecule (one-site states); black, 2h contributions delocalized over two water molecules (two-site states); red, 2h contributions describing one hole on water and one on lithium. Note that several states in the spectra of $(H_2O)_2\oplus$ and $(H_2O)_2Li^+$ are degenerate and that the corresponding lines hide lines of different color. (See the text for details.)

tion of two positive charges created on the water oxygen with a positive charge on lithium amounts to 15.8 eV, twice that of a single oxygen vacancy with a Li^+ ion. The similarity of the overall appearance of the water subspectra of H_2OLi^+ and $H_2O\oplus$ is remarkable, such that all changes in the H_2OLi^+ spectrum may in fact be attributed to the presence of the cationic charge. The increase of the first DIP is thus naturally about twice the increase of the first single-ionization potential (IP). It is indeed noteworthy that for H_2OLi^+ the double-ionization spectrum is subject to a shift of about 8 eV relative to the single-ionization spectrum, compared to the spectra of free water. Because of this, the double-ionization threshold of H_2OLi^+ is much higher than its inner valence ionization energy, whereas both energies are rather similar for the water molecule. Intermolecular electronic decay,[19] namely the relaxation of an ionized state into an energetically lower doubly ionized state, is consequently out of reach following the water inner valence ionization of the H_2OLi^+ cluster. The prerequisite of intermolecular electronic decay following valence ionization is the existence of energetically accessible states in the double-ionization spectrum.

To complete the discussion of H_2OLi^+ ionization, we should address the ionization of the lithium cation. This occurs at significantly higher energies than the water valence ionization but is below the water core ionization. The ionization potential of the lithium cation of H_2OLi^+ is decreased by 3.5 eV compared to a free Li^+. The decrease in the Li^+ ionization energy due to cluster formation is much smaller than the 7-eV increase in the water ionization energy on account of the fact that the destabilization of the Li^+ 1s electrons due to the presence of water is much smaller than the stabilization of the water electrons due the the presence of a positively charged lithium ion. For completeness, we note that, as Figure 1 clearly shows, the states formed by the ionization of the lithium cation are energetically situated above the double-ionization threshold. Therefore, in contrast to the states created by valence ionization of the water molecule, they may undergo electronic decay by spontaneous electron loss. Electronic decay properties of ionized H_2OLi^+ will be discussed elsewhere.[53]

B. Comparing $(H_2O)_2Li^+$ and $(H_2O)_2$: How Geometry Reflects on the Ionization Spectra. Valence ionization and double ionization of $(H_2O)_2Li^+$ are addressed in this subsection. The computed spectra are shown in Figure 2. We discuss first the single-ionization spectrum. Similarly to the spectrum of H_2OLi^+ discussed in the previous subsection, the spectrum of $(H_2O)_2Li^+$ may be divided into a subspectrum related to the water molecules and a subspectrum related to the lithium ion of the cluster. The latter is situated above 68 eV, whereas most of the intensity of the former is situated below 50 eV. The water subspectrum is shifted by 0.7 eV toward lower energies compared to the corresponding H_2OLi^+ subspectrum, and the lithium cation ionization energy is decreased by 3 eV. (See Table 3.) Both water and Li^+ ionization become less difficult when adding an additional water molecule to H_2OLi^+. The electrostatic effects due to the slight variation of the water−lithium distance between the mono- and dihydrated species are small, and the main reason for the relative decrease in the ionization thresholds is found in the electron density distribution. Naturally, the polarizing effect of the lithium cation on each of the two water monomers of $(H_2O)_2Li^+$ is weaker than that on the one water monomer of H_2OLi^+.

TABLE 3: Comparison of the First Ionization Potentials (DIP), the Energy of the Main Line(s) of the Water Inner-Valence Ionization Group (H_2O(iv)-IP), and the Lithium Ionization Potentials (Li(1s)-IP) of Water and the Five Water−Lithium Clusters Investigated

cluster	IP (eV)	DIP (eV)	H_2O(iv)-IP (eV)	Li(1s)-IP (eV)
H_2O	12.85	38.63	33.8	
H_2OLi^+	19.74	53.54	41.0	72.0
$(H_2O)_2Li^+$	19.03	39.52	40.0	69.0
$(H_2O)_3Li^+$	18.06	38.10	39.23	67.4
$(H_2O)_4Li^+$	17.30	36.50	39.0	66.0
$(H_2O)_5Li^+$	16.55	34.95	37.9/38.20/38.3	65.39

To understand the impact of the positive charge, we compare the spectra of $(H_2O)_2Li^+$ to those of $(H_2O)_2\oplus$, a cluster in which a positive point charge replaces the lithium cation. All main characteristics, including the first-ionization potential and DIPs, of the $(H_2O)_2Li^+$ ionization- and double-ionization spectra are well reproduced by the $(H_2O)_2\oplus$ spectra. Finer differences may be visible, however. In particular, the split of the second and third distinguishable lines is more pronounced in the $(H_2O)_2\oplus$ ionization spectrum than in the $(H_2O)_2Li^+$ spectrum.

It is necessary to discuss briefly the composition of the $(H_2O)_2Li^+$ spectrum to understand this energy split. The outer valence ionization energies are given in Table 1. The composition of the spectrum is closely related to the geometry of the cluster. As already discussed in section III, $(H_2O)_2Li^+$ is composed of two water molecules on perpendicular planes on opposite sides of the lithium cation. The first line appearing in the ionization spectrum describes the energetically degenerate ionization of the lone pair on each water molecule that does not interact with the lithium 1s electrons. Because the water molecules are situated in perpendicular planes, these lone pairs are also perpendicular to each other and do not interact. Because the water molecules are symmetrically equivalent, their ionization is energetically degenerate, and only one line is visible in the spectrum. (In Figure 2, the corresponding red line completely hides an identical blue line.) The same picture holds for the fourth visible line of the spectrum, which describes the energetically degenerate ionization from the orbitals involved in OH bonding. The second and third visible lines appear because of the ionization of the remaining lone pairs. Both of these lone pairs point toward the lithium cation such that they may interact with each other giving rise to two energetically distinct states corresponding to the bonding and antibonding combinations. The split between these two states would be nearly negligible in a water dimer (at the same geometry as in the lithium cluster), but it is widened by the polarizing interaction with Li^+ and, even more pronouncedly, with the naked charge in $(H_2O)_2\oplus$. A similar picture holds for the inner valence electrons of water, but here the energy split between the resulting states remains practically negligible.

We now compare the spectra of $(H_2O)_2Li^+$ to those of the water dimer, with the aim of underlining the reflection of the cluster geometry in the spectra. It is obvious that the ionization- and double-ionization spectrum of $(H_2O)_2Li^+$ and $(H_2O)_2$ in its ground-state geometry differ fundamentally (Figure 2 and Table 4). The relative energetic shift of the spectra is explained by the positive charge on the $(H_2O)_2Li^+$ cluster, which is not present in the neutral water dimer. The differences in the overall appearance of the spectra may be explained by the different geometries of the clusters. Whereas the water dimer is known to have a H-donor−acceptor ground-state structure of two water monomers connected by a hydrogen bond, the $(H_2O)_2Li^+$ cluster is composed of two equivalent water molecules, which are both bound to the lithium cation as discussed above. The outer valence ionization spectrum of the water dimer is consequently composed of two sets of lines, each derived from one of the nonequivalent water monomers. The lines of the H-donor (red) are found at lower energies than the corresponding lines of the H-acceptor (blue) water monomer because a larger amount of electron density is localized on the former. The lone pairs that are involved in neither hydrogen bonding nor the OH bonds do not interact in $(H_2O)_2$, so the corresponding lines are completely painted in either red or blue. Small interactions are found for the second lone pair, whereas strong mixing with H-acceptor orbitals is observed for the OH bonding orbital of the H donor. The OH bonding orbital of the H acceptor does not mix with other outer valence orbitals such that the line is completely painted in blue. The inner valence part of the spectrum is composed of two line groups, one representing inner valence ionization of the H-donor monomer and one for the H-acceptor monomer. As we have seen above, the $(H_2O)_2Li^+$ water spectrum shows instead a single set of lines, with the exception of the ionization assigned to the two interacting lone pairs, which is visibly split into two lines by the effect of the Li cation. In agreement with the results for the ionization spectra, the double-ionization spectrum of $(H_2O)_2Li^+$ is composed of fewer distinguishable lines than the double-ionization spectrum of the water dimer (all simple-site states are degenerate). These results emphasize how the cluster geometry may severely influence the appearance of ionization spectra, andphotoelectron spectroscopy may give very helpful information about cluster geometries. The number of nonequivalent monomers, in particular, is crucial in determining the number of lines appearing in ionization and double-ionization spectra.

TABLE 4: Outer Valence Ionization Energies of the $(H_2O)_nLi^+$, $n = 1-5$, Clusters and of the Water Dimer and the Water Molecule Calculated by ADC(3) Green's Function Methods[a]

cluster	state	IP (ev)	cluster	state	IP (eV)
H_2O	^{2}1B$_1$	12.85	$(H_2O)_4Li^+$	^{2}5B$_2$	17.30
	^{2}3A$_1$	15.16		^{2}5B$_3$	17.37
	^{2}1B$_2$	19.11		^{2}6A$_1$	17.73
				^{2}5B$_1$	17.81
$(H_2O)_2$	^{2}2A″	11.91		^{2}4B$_1$	20.17
	^{2}8A′	13.45		^{2}4B$_3$	20.25
	^{2}7A′	14.07		^{2}4B$_2$	20.26
	^{2}6A′	15.84		^{2}5A$_1$	20.81
	^{2}5A′	18.28		^{2}3B$_1$	23.63
	^{2}1A″	19.74		^{2}3B$_3$	23.75
				^{2}4B$_2$	23.78
				^{2}4A$_1$	23.80
H_2OLi^+	^{2}1B$_1$	19.74	$(H_2O)_5Li^+$	^{2}14A	16.55
	^{2}4A$_1$	22.92		^{2}12B	16.86
	^{2}1B$_2$	25.75		^{2}11B	17.17
				^{2}13A	17.18
$(H_2O)_2Li^{+2}$	^{2}1E	19.03		^{2}10B	17.33
	^{2}3B$_1$	21.99		^{2}12A	19.13
	^{2}4A$_1$	22.21		^{2}9B	19.30
	^{2}2E	25.07		^{2}8B	19.81
				^{2}11A	19.99
$(H_2O)_3Li^+$	^{2}4A$_1$	18.06		^{2}10A	20.33
	^{2}3E	18.27		^{2}7B	22.75
	^{2}4E	21.09		^{2}6B	23.34
	^{2}5A$_1$	21.32		^{2}5B	23.40
	^{2}5E	24.32		^{2}9A	23.42
	^{2}1A$_2$	24.33		^{2}8A	23.48

[a] Note that $(H_2O)_4Li^+$ has been calculated in D_2 symmetry, close to S_4 symmetry. The degeneracy of the E states that are found for S_4 symmetry is thus broken, although the corresponding lines are still close in energy.

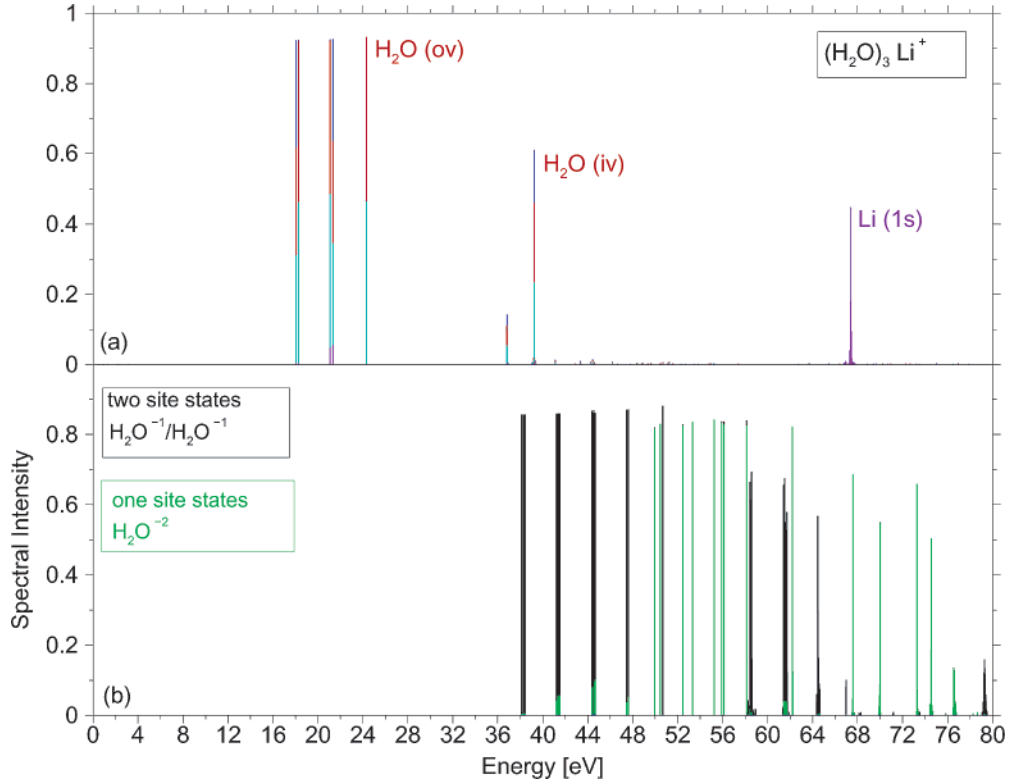

Figure 3. Ionization spectrum (a) and double-ionization spectrum (b) of $(H_2O)_3Li^+$. Coloring of the ionization spectra: blue, 1h contribution localized on one water; red, 1h contribution on a second water; cyan, 1h contribution on the third water molecule; violet, 1h contribution localized on lithium. Coloring of the double-ionization spectra: green, 2h contribution localized on one water molecule (one-site states); black, 2h contribution delocalized over two water molecules (two-site states). Minor Li^+ contributions to the double-ionization spectrum are neglected.

To complete the discussion of $(H_2O)_2Li^+$, we briefly address some aspects of the double-ionization spectrum. A detailed analysis of the double-ionization spectra of all clusters will be presented in section V. In contrast to the few changes in the single-ionization spectra, the differences in the double-ionization spectra of H_2OLi^+ and $(H_2O)_2Li^+$ are dramatic. The double-ionization threshold of the latter is decreased by 14 eV, such that it equals nearly that of an isolated water molecule (cf. the bottom panel of Figure 1 with the double-ionization spectrum of water in Figure 1). This is surprising at first glance because water is a neutral molecule, whereas $(H_2O)_2Li^+$ carries a positive charge and, furthermore, because the single-ionization energies of water are lower than those of $(H_2O)_2Li^+$ by approximately 7 eV. As we shall see in section V, it is the appearance of so-called two-site states, where the two electron vacancies are localized on two different monomers, that is responsible for the surprisingly low first double-ionization energy of $(H_2O)_2Li^+$. The large shift in the double-ionization spectrum of $(H_2O)_2Li^+$ toward lower energies leads to a double-ionization threshold that is in the same energy range as the water inner valence ionization. The expected accuracy limits of our present calculations do not allow us to decide unambiguously whether the electronic decay of the inner valence ionized states by electron loss is energetically accessible. That such a possibility may actually be realized for one of the states, as indicated in Figure 2, is, however, a particularly interesting result. In H_2OLi^+, such a decay is not possible. In the water dimer itself, the inner valence ionization energies are clearly above the double-ionization threshold so that electronic decay is operative in the neutral cluster. As found for H_2OLi^+, the ICD process is undoubtedly operative following Li^+ ionization.

C. Completion of the First Solvation Shell: $(H_2O)_3Li^+$ and $(H_2O)_4Li^+$ Clusters and General Tendencies. The computed single- and double-ionization spectra of the tri- and tetrahydrated lithium ions are shown in Figures 3 and 4, respectively. The outer valence ionization energies are given in Table 4. As we can see, the addition of one or two water monomers to $(H_2O)_2Li^+$ induces a slight decrease in the first- and double-ionization energies. The ionization energy of $(H_2O)_3Li^+$ is smaller by 1 eV compared to its predecessor, and a further decrease of 0.7 eV is computed for $(H_2O)_4Li^+$. The DIP is decreased by 1.5 eV by each additional water monomer. The overall appearance of the single- and double-ionization spectra is not very different from those of $(H_2O)_2Li^+$. The highly symmetric structures of $(H_2O)_3Li^+$ and $(H_2O)_4Li^+$ are reflected in the spectra by the appearance of relatively few line groups, representing the ionization or double ionization of corresponding orbitals of the equivalent monomers. The energy splits and the 1h contributions of the lines in the ionization spectra, which are indicated by the colors in the Figures, are worth a more detailed discussion.

As discussed in the previous subsection, the two water molecules of $(H_2O)_2Li^+$ are situated on perpendicular planes, such that only the lone pairs pointing to the lithium cation interact. Consequently, only one of the water outer valence lines of $(H_2O)_2Li^+$ is split into two lines. The water molecules of $(H_2O)_3Li^+$ and $(H_2O)_4Li^+$ are not perpendicular to each other. Cluster molecular orbitals are therefore formed from all groups of equivalent water outer valence orbitals. Because the relative position of the water molecules of $(H_2O)_3Li^+$ is still rather unfavorable for mutual interaction, the energy split between the lines is very small, and we see in Figure 3 essentially three line clusters that may be illustrated as follows: the HOMO is composed of equivalent contributions from all three lone pairs not pointing to the lithium cation. The corresponding lowest-energy line thus shows all three colors assigned to the different water units. Immediately above this line there is a doubly-

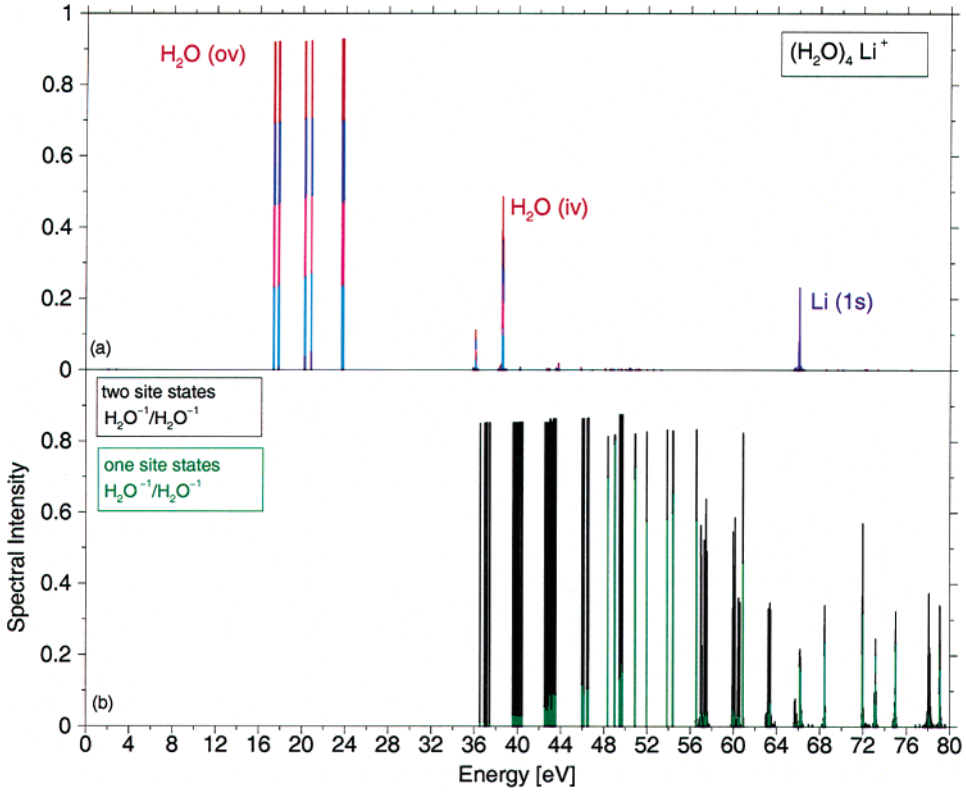

Figure 4. Ionization spectrum (a) and double-ionization spectra (b) of $(H_2O)_4Li^+$. Coloring of the ionization spectra: blue, 1h contribution localized on one water; red, 1 h contribution on a second water; cyan, 1h contribution on a third water molecule; magenta, 1h contribution on the forth water molecule; violet, 1h contribution localized on lithium. Coloring of the double-ionization spectra: green, 2h contribution localized on one water molecule (one-site states); black, 2h contribution delocalized over two water molecules (two-site states). Minor Li^+ contributions to the double-ionization spectrum are neglected. Note that some of the lines in the double-ionization spectrum are degenerate.

degenerate line corresponding to the other two linear combinations derived from the same lone pairs. Each includes one nodal plane in addition to the nodal planes due to the p character of the lone pairs. The single line appearing in the spectrum, which hides its degenerate companion, shows equivalent contributions from two of the lone pairs. The third water monomer is situated in the nodal plane, and the hidden line is mainly composed of the contribution of this third water monomer's lone pair. The second and third clusters of lines are similarly explained, but they refer to the lone pairs pointing to the lithium cation and to the states describing OH bonding, respectively. In the latter case, the split between the singly- and doubly-degenerate lines is practically undetectable. One may notice that for the second group of states the order of the ionization lines is reversed: the line due to the state with equivalent contributions from all water monomers is found at a higher energy than the doubly-degenerate line. This reversal also occurs for the third group of states, although, as noted here, the split is nearly vanishing. Finally, the inner valence states are composed in a similar manner to the outer valence ones, but here too their energy gap is nearly zero and only the (broken down) line with equally distributed 1h contributions shows.

The relative orientation of the orbitals of different water monomers of $(H_2O)_4Li^+$ is such that their interaction is stronger than in $(H_2O)_3Li^+$. The energy splits between the corresponding outer valence lines are therefore slightly larger. The ionization from the first group of lone pairs is represented by two nearly doubly-degenerate lines. The remaining lone pairs are represented by one approximately triply-degenerate line and one line describing their all-bonding interaction. The lines due to the orbitals involved in OH bonding are not resolved. All valence lines are composed of equal contributions from each of the water molecules because of the cluster symmetry. The lines of the inner valence subspectrum, which are set up in the same way, are not resolved.

The double-ionization threshold in the tri- and tetrahydrated clusters is computed to lie farther in energy to the water inner valence single-ionization lines than we found for $(H_2O)_2Li^+$ (Table 3). Thus, although the accuracy of the present calculations still does not permit a definitive statement, it seems likely that in the two larger clusters at least some of the inner valence ionized states lie above the double-ionization edge so that their decay via electron loss can take place. As for the other clusters, in $(H_2O)_{3,\,4}Li^+$ the Li 1s ionization is clearly above the double-ionization threshold so that molecular electronic decay is operative. It will be addressed elsewhere.[53]

In the following text, we discuss the changes in ionization and double-ionization energies taking place upon increasing the number of water molecules from $n = 1-4$, thereby completing the first solvation shell. The opening of the second solvation shell is also briefly addressed. It will be discussed in detail in section VI.

As observed above, the DIP and the inner valence ionization energy both decrease with an increasing number of water molecules in the cluster. After the second water unit is added, which opens the possibility of the creation of dicationic two-site states, the DIP decreases by about 1.5 eV for each further water addition. The decrease of the water inner valence ionization potential slows down from 1 to 0.2 eV from $n = 1-4$. The opening of the second solvation shell, which will be discussed in detail later on, leads to a further decrease of the water inner valence ionization energy by 1.1 eV. The ionization threshold of the clusters decreases rather constantly by 0.8 eV for each water molecule added from one to five. The constant

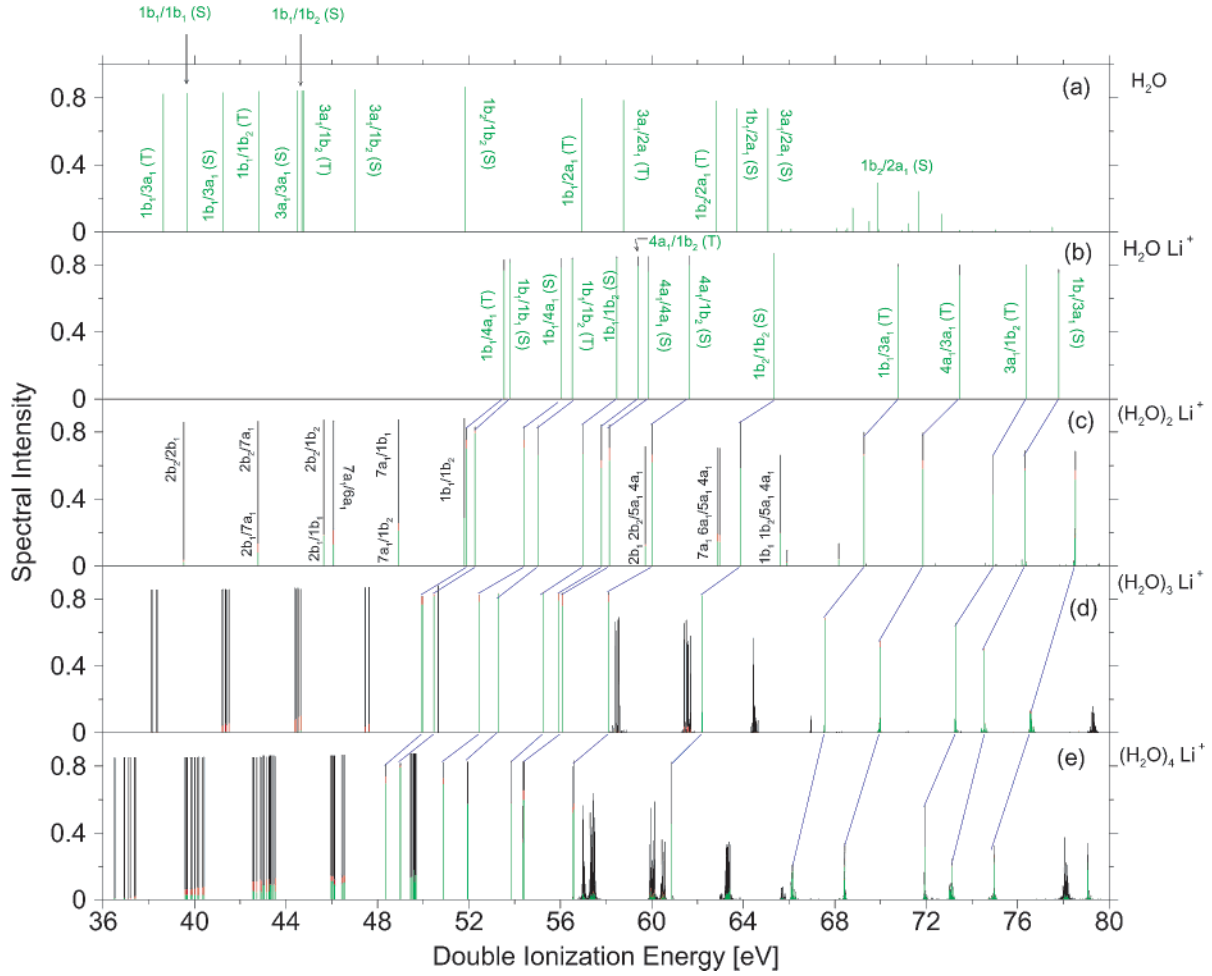

Figure 5. Comparison of the water double-ionization spectrum (a) and the double-ionization spectra of $(H_2O)_nLi^+$. (b−e): $n = 1, 2, 3, 4$. Coloring: green, 2h contributions localized on one water molecule (one-site states); black, 2h contribution delocalized over two water molecules (two-site states); red, 2h contribution describing one hole on water and one on lithium. The leading 2h contribution of the (one-site) states in the spectra of water and H_2OLi^+ and the two-site states in the spectrum of $(H_2O)_2Li^+$ are assigned to the contributing molecular orbitals. The notation orbital1 orbital2/orbital3 orbital4 is a short term for 2h contribution of various pairs orbital 1/orbital 3, orbital 1/orbital 4, orbital 2/orbital 3, and orbital 2/orbital 4 to four energetically degenerate lines. Note that most of the one-site states and many two-site states are degenerate. T and S stand for triplet and singlet dicationic states.

decrease of the DIP, which is in the range of twice the decrease of the ionization potential, is thus simply explained by the fact that the effect of partial charge reduction plays a role twice. We should note here that not only the ionization threshold but also the water outer valence subspectra are shifted with an increasing number of water monomers in the cluster.

Interestingly, the change in the lithium ionization energy follows a different pattern from that of the water outer valence ionization energy discussed above. The lithium ionization energy also decreases with cluster size, but it shows a tendency to stabilize, that is, decrease less and less. This result may be explained as follows: the strong polarizing effect of the lithium cation causes the partial transfer of positive charge to the water molecule of H_2OLi^+. The total amount of charge transferred from lithium increases with the number of water molecules (causing the observed decrease in the Li^+ IP) but of course less than linearly: each particular water molecule hosts a smaller portion of the electron hole as the cluster size increases, until saturation is achieved. Furthermore, when the second solvation layer starts to form with the fifth water molecule, there is no longer direct bonding between lithium and the added water molecules so that the IP remains essentially stable. By contrast, the further shift in the water ionization spectrum after the completion of the first solvation shell lies in the charge redistribution via direct water−water interaction between the different shells. This point will be addressed again in section VI.

V. Analysis of Double-Ionization Spectra of $(H_2O)_nLi^+$, $n = 1-4$

A detailed comparison of the double-ionization spectra of the water molecule and the clusters of the first solvation shell is depicted in Figure 5. All lines shown can be related to one or two water molecules, as will be discussed in detail in the following text. Upon adding a lithium cation to a water molecule to obtain the H_2OLi^+ cluster, the first double-ionization energy increases substantially by approximately 15 eV, from 38.63 to 53.54 eV. This shift toward higher double-ionization energies is nearly compensated by a shift to lower energies when an additonal water molecule is added to H_2OLi^+ to obtain the $(H_2O)_2Li^+$ cluster. The first DIP decreases from 53.54 eV for H_2OLi^+ and to 39.52 eV for $(H_2O)_2Li^+$. Water and $(H_2O)_2Li^+$ have thus very similar DIPs, although their IPs differ by more than 6 eV. This remarkable result may be rather surprising at first sight but is easily explained. The lowest double ionization of the H_2OLi^+ cluster corresponds essentially to removing two electrons from the HOMO of the water molecule. The HOMO double-ionization energy of H_2OLi^+ is shifted by 15 eV to

higher energies with respect to the corresponding water HOMO double-ionization energy because of the repulsion of the resulting double hole charge with the charge of the lithium cation. By stark contrast, the lowest double-ionization energy of $(H_2O)_2Li^+$ does not originate from the double ionization of a single water molecule. It is due to the creation of one hole in the HOMO of each of the two available water units. Both holes still have a repulsive interaction with the lithium cation, but their mutual repulsion is strongly decreased by distance. The energy gain by hole localization on two monomers at a distance of 3.7 Å, in comparison to the repulsion energy of the two holes in the HOMO of one monomer, is as large as 14 eV. This turns out to be similar to the repulsive interaction energy of a double hole with a lithium cation at a distance of 1.8 Å. The fact that adding another water molecule to H_2OLi^+ approximately compensates the repulsion due to the lithium ion may be used to estimate the energy of the hole−hole repulsion at one water molecule according to

$$E_{\text{repulsion}}(H_2O^{+\leftrightarrow+}) \approx E_{\text{repulsion}}(H_2O^{++} \leftrightarrow Li^+)_{r=1.85} + E_{\text{repulsion}}(H_2O^+ \leftrightarrow H_2O^+)_{r=3.70} \approx 19.5 \text{ eV}$$

The DIPs of the $(H_2O)_3Li^+$ and $(H_2O)_4Li^+$ clusters are further decreased compared to the DIP of $(H_2O)_2Li^+$. The decrease due to the third and fourth water molecule is marginal compared to the effect of the second water molecule. As discussed above, the addition of a second water molecule to H_2OLi^+ decreases the DIP by approximately 15 eV, whereas each of the third and fourth added water molecules leads to a further decrease by approximately 1.5 eV (Table 3). The reason for the strong impact of the addition of a second water molecule is the possibility of localizing the two hole charges on two different monomers (two-site states). The third and fourth monomers add more two-site states (and one-site states) to the already existing states but do not change the character of the states in the double-ionization spectrum. The impact of monomers 3 and 4 on the DIP is thus small and of a different nature. It is explained by the decrease of the positive partial charge on the water monomers with an increasing number of water monomers in the cluster.

We will now analyze the composition and the energetic shifts of the double-ionization spectra of $(H_2O)_{1-4}Li^+$ aqueous cationic clusters in detail and relate them to the results for water. The water double-ionization spectrum is shown for comparison in part a of Figure 5. The assignment of the lines in this spectrum is rather straightforward because we know the irreducible representation of each dicationic state. The line ordering simply reflects the energetics of the molecular orbitals obtained from the Hartree−Fock calculation and the hole−hole repulsion. All lines assigned to holes in two different MOs are shifted by approximately 12 eV with respect to the sum of the two Hartree−Fock molecular orbital energies. Lines assigned to a double ionization from one orbital show an additional shift of ∼2 eV. Furthermore, all lines assigned to holes on two different MOs are split into a singlet and an energetically lower-lying triplet line, indicated by S and T, respectively. The triplet/singlet split is in the range of 2.5 eV for ov/ov lines and in the range of 6 eV for ov/iv lines. The large split of iv/ov lines in comparison to that of ov/ov lines is explained by the spatial compactness of the inner valence orbital densities and their proximity to the outer valence orbitals compared to the mutual ov/ov main electron density distance. The ov/ov part of the water double-ionization spectrum is separated from the ov/iv part of the spectrum by a gap of ∼5.5 eV. The iv/ov water double-ionization spectrum begins at 57 eV (Figure 5a). All lines in the water valence double-ionization spectrum are dominated by their 2h contributions, except for the $1b_2/2a_1$(S) line, which shows significant breakdown characteristics due to 3h1p contributions.

Below 102.6 eV, the double-ionization spectrum of the H_2OLi^+ cluster is essentially the spectrum of the water ligand (shown only up to 80 eV in Figure 5b). At 102.6 eV, the first H_2O^{-1}/Li^{-1} line is observed. The part of the spectrum shown may thus be analyzed as a modified double-ionization spectrum of water. The assignment of the lines to their respective dominant 2h contributions may be simply derived with the help of the irreducible representation of the respective lines and the analysis of the orbital energies. Apart from the shift of about 15 eV discussed above, the ordering of the lines in terms of their 2h character remains unchanged for most of the lines as compared to that of water. Nevertheless, the H_2OLi^+ and the water spectra appear to be rather different at first sight because of different energy gaps between some of the lines. The relative line shifts are essentially explained by a stronger influence of the positive charge on lithium on the $4a_1$ orbital than on the other outer valence orbitals. The lines with $4a_1$ hole contributions are thus shifted by ∼1 eV to higher energies relative to the other lines. The $4a_1/4a_1$ line is consequently subject to a larger relative shift of ∼2 eV. This also changes the order of the fifth, sixth, and seventh lowest-lying lines. In the free-water spectrum, these lines are, respectively, due to $^1 3a_1/3a_1$, $^1 1b_1/1b_2$, and $^3 3a_1/1b_2$, and they are nearly degenerate. The influence of Li^+ on the outer valence a_1 MO in H_2OLi^+ perturbs this near degeneracy and changes the order of the lines to $^1 1b_1/1b_2$ (which has no relative shift), $^3 4a_1/1b_2$ (single relative shift), and $^1 4a_1/4a_1$ (double relative shift). (Note that the $2a_1$ of the H_2OLi^+ cluster is identified with the lithium 1s orbital.) The sequence of all other lines is unchanged.

The double-ionization spectra become much more complex when more than one water molecule binds to Li^+. In $(H_2O)_2Li^+$, the lowest line involving the ionization of lithium is found at 94.1 eV, below which the spectrum is essentially composed of water lines. Figure 5c depicts a part of this spectrum. Green contributions to the lines denote H_2O^{-2} character, where both hole charges are localized at the same water molecule (one-site states). Black contributions denote H_2O^{-1}/H_2O^{-1} contributions, where each hole is localized at a different water molecule (two-site states). The latter states are naturally energetically more favorable than the H_2O^{-2} states because of the lack of intramolecular hole repulsion. In contrast to the one-site states, the energy split between triplet and singlet two-site states is mostly too small to be detected in the Figure because the distance between the interacting holes on different monomers is large. Below 51.90 eV, only lines dominated by two-site contributions are found, and in fact, all two-site ov/ov lines of the $(H_2O)_2Li^+$ cluster are found in the interval from 39.53 to 51.80 eV. Interestingly, these lines thus lie below all one-site states. In this interval, the order of the two-site states reflects the energetics of the molecular orbitals, and the double-ionization energies are very similar to those expected from the sum of the Hartree−Fock energies of the orbitals involved. The ov/iv two-site states are found in the interval from 59.71 to 65.61 eV. They are embedded in the ov/ov one-site double-ionization spectrum. The order of the iv/ov two-site states is also found to match the spectrum expected from the analysis of the Hartree−Fock MOs. However, unlike the energies of ov/ov two-site states, the energies of the iv/ov two-site states differ significantly from the values expected from the Hartree−Fock

calculation. The energy difference between the calculated double-ionization energies and the Hartree−Fock energies is in the range of 3 eV. The reason for this shift is the increasing impact of electron correlation in the inner valence region.

The part of the double-ionization spectrum of $(H_2O)_2Li^+$ that is assigned to one-site states begins at 51.90 eV, slightly above the highest-lying ov/ov two-site line. All of the lines are readily assigned to their respective 2h contributions by comparison with the H_2OLi^+ spectrum. With respect to the latter, the energies of the one-site states are smaller by ∼1.5 eV. The shift arises from the possibility of a more favorable charge redistribution in the cluster with two water molecules compared to a cluster with only one water molecule. The complex double-ionization spectrum of the $(H_2O)_2Li^+$ cluster is thus readily understood once its composition in terms of one-site states and two-site contributions is revealed. It should be added here that the spectrum is expected to be much more complex if the D_{2d} symmetry of the $(H_2O)_2Li^+$ cluster is broken. The relatively small number of lines in the spectrum analyzed here is a consequence of the symmetry equivalence of the two water monomers.

The double-ionization spectrum of $(H_2O)_3Li^+$ is shown in part d of Figure 5. It also reflects the highly symmetric geometry of the cluster, which is composed of three equivalent water monomers. The spectrum is characterized by distinct groups of lines that may be assigned to the 2h contributions by comparison with those in the spectrum of $(H_2O)_2Li^+$, which shows similar structures. The correspondence among one-site lines in the two spectra is made evident by connecting blue lines. Corresponding lines describing two-site states may be assigned in a similar manner to the one-site states.

In contrast to the HOMOs of the two water molecules of the $(H_2O)_2Li^+$ cluster, the HOMOs of the water monomers of $(H_2O)_3Li^+$ are not perpendicular to each other. Consequently, their interaction leads to the formation of three states, two of which are degenerate. Whereas one line appears because of a HOMO two-site double ionization of $(H_2O)_2Li^+$, two singlet lines and two triplet lines are present in the spectrum of $(H_2O)_3Li^+$, one line of each multiplicity being doubly degenerate. The interpretation of the multiple groups of lines for the remaining two-site states with large 2h contributions (below 52 eV) is similar. Additional effects must be taken into account to explain the very complicated two-site line groups above 54 eV. They are situated above the triple-ionization threshold such that they may undergo electronic decay to triply-ionized states. The line broadening due to decay appears as line bundling in our discrete calculations.[19] The electronic decay properties of the states in the double-ionization spectrum will be discussed elsewhere.[53]

In comparison to the one-site states in the spectrum of $(H_2O)_2Li^+$, the one-site states in the double-ionization spectrum of $(H_2O)_3Li^+$ are all shifted by ∼1.5 eV. Because the two-site states are shifted only by ∼1 eV toward smaller energies, the one-site and the two-site spectra now overlap slightly, with two of the line groups belonging to the one-site spectrum lying below the highest ov/ov two-site group. The shift of the double ionization lines observed upon adding a water monomer to $(H_2O)_2Li^+$ is due to the smaller positive charge on each water monomer. The reduction of this positive charge has a stronger impact if the two holes are localized on the same monomer (one-site states) than in the two-site states so that the shift of the two-site states is slightly smaller than that of the one-site states.

The spectrum of $(H_2O)_4Li^+$ may be analyzed in a similar manner to that of $(H_2O)_3Li^+$. It is obviously composed of groups of one-site states and two-site states, indicated by green and black lines in Figure 5e. Their ordering is similar to the ordering of the corresponding groups for $(H_2O)_3Li^+$. The energy of the two-site states in the $(H_2O)_4Li^+$ spectrum decreases by ∼1 eV relative to their counterparts in $(H_2O)_3Li^+$. The shift of the one-site states is slightly larger, as explained for the smaller clusters. Like its smaller analogues, the $(H_2O)_4Li^+$ cluster is also composed of next-to-equivalent water molecules (D_2 symmetry, close to S_4 symmetry). The $(H_2O)_4Li^+$ one-site double-ionization spectrum is thus composed of four overlaying shifted water spectra. The two-site subspectrum is composed of several line groups originating from 2h contributions of similar character, corresponding to states of slightly different energies. The same kind of energy splitting has already been described above for the lowest-lying group in the $(H_2O)_3Li^+$ double-ionization spectrum.

The double-ionization spectra of H_2O, H_2OLi^+, and $(H_2O)_2Li^+$ below 80 eV are composed of lines with high intensity and 2h character. By contrast, as mentioned above, the two-site lines above 56 eV and the one-site lines above 76 eV in the spectrum of $(H_2O)_3Li^+$ are characterized by line bundles composed of low-intensity lines. A similar phenomenon is observed for the one-site lines above 66 eV of the spectrum of $(H_2O)_4Li^+$. As we have said, this line splitting and bundling indicates that the corresponding lines are above the triple-ionization threshold and that the states may decay electronically to form triply-ionized states. For a general discussion of why the splitting and clustering of lines in the double-ionization spectrum is indeed caused by electronic decay and its implications, refs 53 and 54.

VI. Opening the Second Solvation Shell: Results for the $(H_2O)_5Li^+$ Cluster

The usual coordination number of the lithium cation in the first solvation shell is four so that the second solvation shell is opened in the $(H_2O)_5Li^+$ cluster. In the following text, the ionization and the double-ionization spectra of $(H_2O)_5Li^+$ are discussed, and the impact of the second solvation shell monomer on them is addressed in particular.

We will adopt the following nomenclature for the discussion of the spectra, which are reported in Figure 6. According to the picture of $(H_2O)_5Li^+$ also shown in the Figure, those water molecules that are directly bound to the lithium cation but not to the fifth water molecule are referred to as water A. The water molecules directly bound to the lithium cation and bound to the fifth water molecule by hydrogen bonding are referred to as water B, whereas the water molecule of the second solvation shell is referred to as water C.

We address the double-ionization spectrum first. The double-ionization spectrum of $(H_2O)_5Li^+$ appears much less well ordered and therefore much more complex than the corresponding spectra of the first solvation shell clusters. It is composed of dense-lying lines, which may not be assigned to their dominating 2h components by comparison to spectra of smaller clusters. For the $(H_2O)_5Li^+$ spectrum, the assignment of each line should be done individually by analyzing its eigenvector components. The reason for the complicated double-ionization spectrum is mainly the presence of nonequivalent water monomers in the cluster. The relatively small energy differences between the three different types of water molecules destroy the highly ordered spectrum found for the predecessor $(H_2O)_4Li^+$. It is noted here that the $(H_2O)_5Li^+$ ground-state geometry may still be considered to be rather symmetric for a system of its size. Even more complicated spectra result for unsymmetric

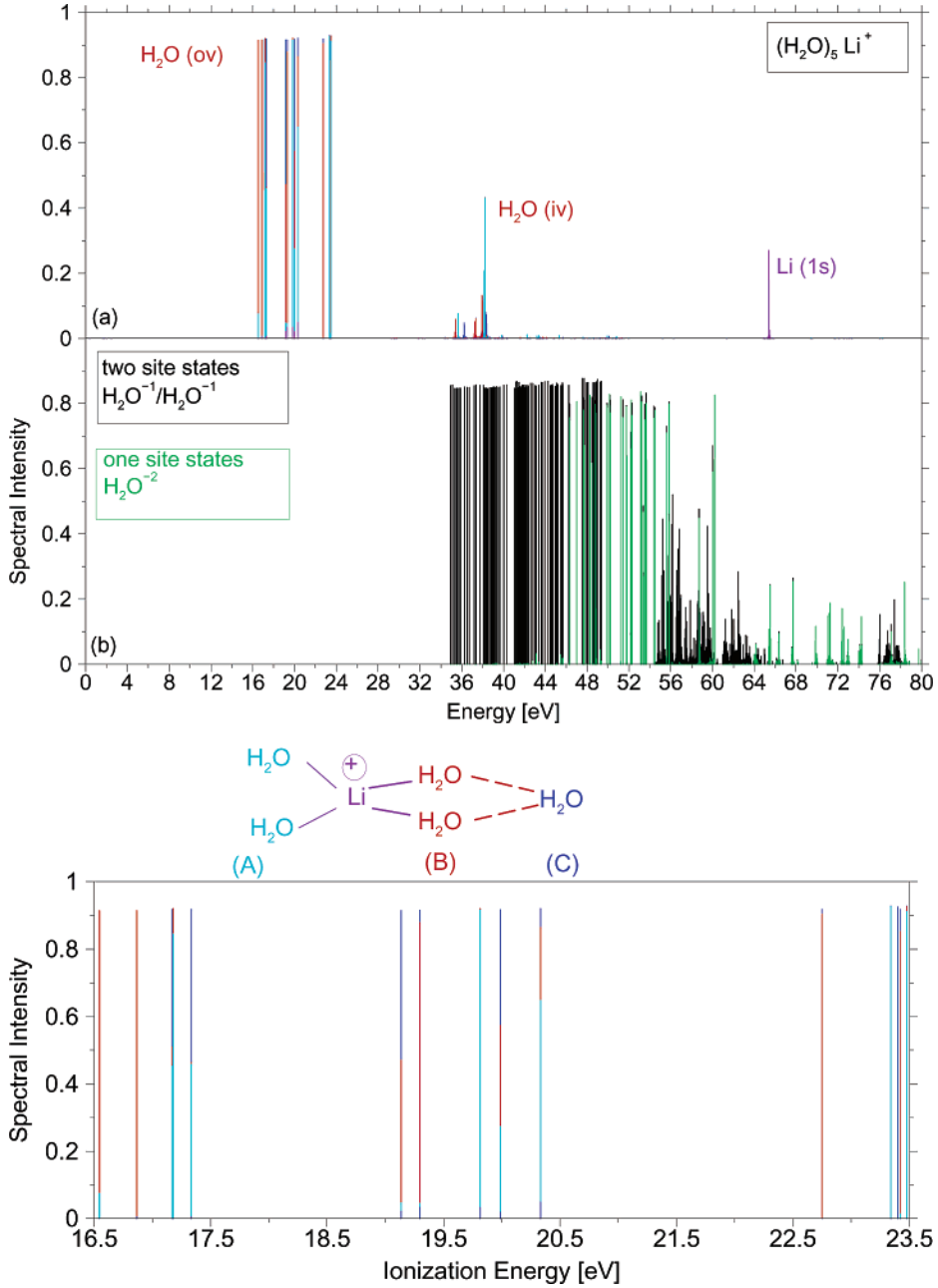

Figure 6. (Top) ionization spectrum (a) and double-ionization spectrum (b) of $(H_2O)_5Li^+$. (Bottom) enlarged water outer valence ionization spectrum of $(H_2O)_5Li^+$. Coloring of the ionization spectra: blue/red/cyan, 1h contribution localized on water molecules shown with the respective colors; violet, 1h contribution localized on lithium. Coloring of the double-ionization spectra: green, 2h contribution localized on one water molecule (one-site states); black,2h contribution delocalized over two water molecules (two-site states). Minor Li^+ contributions to the double-ionization spectrum are neglected.

ground-state geometries of similarly large molecules or clusters. It is thus justified to conclude that double-ionization spectra are very sensitive to structure and that they may be very helpful in discriminating among different hypotheses for ground-state geometries.

Although we do not assign particular lines of the $(H_2O)_5Li^+$ double-ionization spectrum, it is interesting to discuss briefly its basic composition. We address the two-site states first. The lowest-lying states of the spectrum are characterized by one hole at a water A molecule and one hole localized on water C. This result is in agreement with the minimization of hole repulsion expected for the lowest-lying states of the double-ionization spectrum. The A/C two-site states are energetically followed by A/B and B/B two-site states, which are more favorable than A/A and B/C two-site states because of the lower monomer ionization energies, as will be discussed below. The energy differences between corresponding lines are small. This composition principle is obeyed for the whole two-site subspectrum. The energetically lowest one-site states are characterized by 2h contributions on water B, followed by waters A and C. This energy sequence is in agreement with the ionization spectrum, as we shall now discuss.

The energy shift of the $(H_2O)_5Li^+$ ionization spectrum (and also of the double-ionization spectrum) with respect to the $(H_2O)_4Li^+$ spectrum is not substantially different from the corresponding shifts calculated for the lower members along the series. This result is easily understood once one realizes that the first-ionization energy of all clusters involves water molecules in the first solvation shell, but this is not an obvious finding. In view of the larger IP of the first solvation layer

compared to that of free water and the weaker electrostatic force acting on the second layer, a much smaller first-ionization energy due to second solvation shell ionization accompanied by smaller shifts of the first shell-ionization energies would have been plausible as well. Clearly, the interaction of the water molecule in the second solvation shell with the rest of the cluster via hydrogen bonding has an important influence on the electron density distribution of the cluster. The effect of this is also seen in the water inner valence subspectrum. Here, the line clusters corresponding to ionization of the three nonequivalent types of water monomers are resolved in the spectrum, underlining the influence of the cluster symmetry. All three groups show pronounced line bundling indicating that molecular electronic decay is operative for these states as well as lithium (1s) ionization. The molecule in the second solvation shell is ionized at higher energies than the molecules of the first solvation shell. The formation of the second solvation shell thus decreases the ionization energies of the first solvation shell, at the expense of higher ionization energies of the second solvation shell.

When analyzing in greater detail the outer valence ionization spectrum, we find that the lowest energy corresponds to the ionization of one of the equivalent water molecules that are hydrogen bonded to the second solvation shell. The energy split between the antibonding and bonding linear combination of water B lone pairs is quite large. The outer valence ionization energies of the water molecules A that are directly bound to the lithium cation and the water molecule C of the second solvation shell are rather similar and are higher than the water B first ionization. Two of the lines due to water A ionization, the bonding and the antibonding linear combinations of the lone pairs mixed with some water C contributions, are not resolved in Figure 6. One would expect the same line ordering for the second group of lone pairs and for the orbitals involved in OH bonding. This is not exactly the case. Concerning the group of lines related to the ionization of the inner lone pairs, we find that the bonding state of water B molecules has antibonding contributions from water C such that its ionization energy is unexpectedly lower than that of the (nearly pure) water B antibonding state. The latter is followed by water A ionization from the antibonding state as expected. The corresponding bonding state is found at higher ionization energies because it interacts with the lithium cation. Water C ionization, strongly mixed with water B and A contributions, appears therefore at smaller energies. Interaction with the lithium cation also explains the unexpectedly high ionization energies of the bonding states of water B and A in the OH bond region. They are shifted above water C ionization such that a relatively large energy gap appears between them and the water B antibonding line.

Having analyzed the properties of the smallest cluster of the second solvation shell, we find it interesting to discuss how they are expected to evolve with an increasing number of water molecules in the second and higher solvation shells. Because the most stable isomer of $(H_2O)_6Li^+$ has a structure that is rather close to that of $(H_2O)_5Li^+$, similar ionization energy patterns can be expected. The $(H_2O)_6Li^+$ ground-state structure is characterized by two equivalent water molecules that are hydrogen bonded to two B-type water monomers without involving the water A-type monomers very much. In the context of valence ionization energies of different types of water molecules in the cluster, it is interesting to study whether the ionization of the second solvation shell is energetically more demanding than that of the first solvation shell in general. The effect of charge transfer to a particular water molecule of the second solvation shell via the hydrogen bond is expected to be smaller when a larger number of water molecules is present in the second solvation shell. An increasing number of water molecules and especially the inclusion of additional solvation shells can therefore be expected to lead to closer-lying ionization energies of the individual water units within a solvation shell (which tend to become essentially equivalent) and also to closer-lying ionization energies of different solvation shells.

VII. Conclusions

We have analyzed the ionization and double-ionization spectra of the series of $(H_2O)_nLi^+$ ($n = 1-5$) clusters calculated ab initio by Green's function methods. The results for different clusters were intercompared and compared to water ionization with the aim of studying the influence of microsolvation on the spectra.

Concerning the influence of microsolvation in general, we showed that the changes in the spectra with respect to those of a free water molecule are largely explained by the mere presence of the positive charge. The single-ionization spectra are shifted in energy by ~8 eV, and the double-ionization spectra, by ~15 eV. All main lines are essentially equally shifted, with only minor relative shifts of some valence lines. Intercomparing the energetics of the $(H_2O)_nLi^+$ spectra, we found moderately decreasing first-ionization energies with an increasing number of water monomers in the cluster due to the redistribution of the cationic charge. The overall appearance of the ionization spectra, in particular, the number of outer valence lines that are resolved, is predominantly determined by the cluster symmetry. The symmetry of the cluster ground-state geometry determines the number of nonequivalent water molecules. The total number of water molecules in the cluster is less important than the number of nonequivalent water molecules in determining the overall appearance of the spectra. An instructive example of this fact is the comparison of $(H_2O)_2Li^+$ and $(H_2O)_2$ spectra. A second example is the $(H_2O)_5Li^+$ cluster, for which the high symmetry of the predecessor $(H_2O)_4Li^+$ is broken by the presence of the second solvation shell monomer. The resulting spectra are much less well ordered and become rather complex in comparison.

The composition of all first solvation shell clusters' ionization spectra was discussed in detail with respect to assigning all outer valence lines. It is revealed that the relative orientation of the water molecules determines the energy splits between corresponding lines because it influences the interaction of corresponding monomer orbitals.

Concerning the double-ionization spectra of the first shell aqueous microsolvation clusters of the lithium cation, we showed that the rather complicated spectra of the larger first solvation shell clusters may be decomposed and understood by the help of the smaller clusters' spectra. As soon as two or more water monomers are present in the cluster, the double-ionization spectra are composed of a two-site state subspectrum, which includes those states where the two holes are located on two different water monomers of the cluster and a one-site state subspectrum. The latter comprises all states with both holes localized on one monomer of the cluster. The assignment of the lines is facilitated by the high symmetry of the clusters leading to few well-separated groups of lines with similar hole characteristics. The relatively regular composition of the double-ionization spectra is broken by the partial formation of the second solvation shell in $(H_2O)_5Li^+$ because of the fact that the water molecules are no longer equivalent. The overall appearance of the double-ionization spectrum turns out to be very sensitive to cluster symmetry.

Including a monomer of the second solvation shell in the cluster, double- and single-ionization spectra thus become more complicated. It was discussed, in particular, for the single-ionization spectrum, that the hydrogen-bonded molecule of the second solvation shell severely influences the properties of the water molecules in the first solvation shell; in particular, it facilitates the ionization of its neighboring monomers. Consequently, the water monomer in the second solvation shell has a comparatively high ionization energy (higher than the first solvation shell ionization energies). The impact of the hydrogen bond on the cluster electron density distribution is thus revealed by analyzing the cluster ionization and double-ionization spectrum. For future work, it will be most interesting to determine if this effect of the hydrogen bond is maintained or decreased by adding additional water molecules to the second solvation shell.

Summarizing the results of this contribution, we have shown how not only structural properties such as cluster ground-state symmetries and mutual monomer orientation but also cluster bonding properties are reflected in ionization and double-ionization spectra. Ionization and double-ionization spectra may thus be considered to be very useful for the study of microsolvation clusters.

Acknowledgment. Financial support by the Graduiertenkolleg "Complex Processes: Modeling, Simulation and Optimization" at the Interdisciplinary Center for Scientific Calculation (IWR) at the University of Heidelberg (I.B.M.) and by the DFG (L.S.C.) is gratefully acknowledged.

References and Notes

(1) Hartke, B.; Charvat, A.; Reich, M.; Abel, B. *J. Chem. Phys.* **1997**, *116*, 3588.
(2) Liu, K.; Cruzan, J. D.; Saykally, R. J. *Science* **1996**, *271*, 929.
(3) Jorgensen, W. L.; Severance, D. L. *J. Chem. Phys.* **1993**, *99*, 4233.
(4) Watts, R. O.; Clementi, E.; Fromm, J. *J. Chem. Phys.* **1974**, *61*, 2550.
(5) Clementi, E.; Barsotti, R. *Chem. Phys. Lett.* **1978**, *59*, 21.
(6) Koneshan, S.; Rasaiah, J. C. *J. Chem. Phys.* **2000**, *113*, 8125.
(7) Barnett, R. N.; Landman, U. *J. Phys. Chem.* **1996**, *100*, 13950.
(8) Dang, L. X. *J. Chem. Phys* **1992**, *96*, 6970.
(9) Perera, L.; Berkowitz, M. L. *J. Chem. Phys.* **1991**, *95*, 1954.
(10) Feller, D.; Glendening, E. D.; Kendall, R. A.; Peterson, K. A. *J. Chem. Phys.* **1993**, *100*, 4981, and references therein.
(11) Yamabe, S.; Kuono, H.; Matsumura, K. *J. Phys. Chem. B* **2000**, *104*, 10242.
(12) Bauschlicher, C. W., Jr.; Langhoff, S. R.; Partridge, H.; Rice, J. E.; Komornicki, A. *J. Chem. Phys.* **1991**, *95*, 5142.
(13) Tanaka, H.; Yokoyama, K.; Kudo, H. *J. Chem. Phys.* **2000**, *113*, 1821.
(14) Tanaka, H.; Yokoyama, K.; Kudo, H. *J. Chem. Phys.* **2001**, *114*, 152.
(15) Schultz, J. A.; McLean, W.; Petersen, L.; Jarnagin, R. C. *Chem. Phys. Lett.* **1979**, *64*, 230.
(16) Koch, E.-E.; Sasaki, T.; Winick, H. *Handbook of Synchrotron Radiation*; North-Holland: Amsterdam, 1987.
(17) Kimura, K.; Katsumata, S.; Achiba, Y.; Yamazaki, T.; Iwata, S. *Handbook of HeI Photoelectron Spectra of Fundamental Organic Molecules*; Halsted: New York, 1981.
(18) Cederbaum, L. S.; Domcke, W.; Schirmer, J.; von Niessen, W. *Adv. Chem. Phys.* **1986**, *65*, 115.
(19) Cederbaum, L. S.; Zobeley, J.; Tarantelli, F. *Phys. Rev. Lett.* **1997**, *79*, 4778.
(20) Zobeley, J.; Cederbaum, L. S.; Tarantelli, F. *J. Chem. Phys.* **1998**, *108*, 9737.
(21) Zobeley, J.; Cederbaum, L. S.; Tarantelli, F. *J. Phys. Chem. A* **1999**, *103*, 11145.
(22) Santra, R.; Zobeley, J.; Cederbaum, L. S.; Moiseyev, N. *Phys. Rev. Lett.* **2000**, *85*, 4490.
(23) Santra, R.; Zobeley, J.; Cederbaum, L. S. *Phys. Rev. B* **2001**, *64*, 245104.
(24) Zobely, J.; Santra, R.; Cederbaum, L. S. *J. Chem. Phys.* **2001**, *115*, 5076.
(25) Marburger, S.; Kugeler, O.; Hergenhahn, U.; Möller, T. *Phys. Rev. Lett.* **2003**, *90*, 2023401.
(26) Fetter, A. L.; Walecka, J. D. *Quantum Theory of Many-Particle Systems*; McGraw-Hill: New York, 1971.
(27) Cederbaum, L. S.; Domcke, W. *Adv. Chem. Phys.* **1977**, *36*, 205.
(28) Linderberg, J.; Öhrn, Y. *Propagators in Quantum Chemistry*; Academic: London, 1973.
(29) Öhrn, Y.; Born, G. *Adv. Quantum Chem.* **1981**, *13*, 1.
(30) Ortiz, J. V. In *Computational Chemistry: Reviews of Current Trends*; Leszcyinski, J., Ed.; World Scientific: Singapore, 1997;Vol. 2, p 1.
(31) Schirmer, J.; Cederbaum, L. S.; Walter, O. *Phys. Rev. A* **1983**, *28*, 1237.
(32) Schirmer, J.; Angonoa, G. *J. Chem. Phys.* **1989**, *91*, 1754.
(33) Weikert, H.-G.; Meyer, H.-D.; Cederbaum, L. S.; Tarantelli, F. *J. Chem. Phys.* **1996**, *104*, 7122.
(34) Schirmer, J.; Barth, A. *Z. Phys. A: Hadrons Nucl.* **1984**, *317*, 267.
(35) Gottfried, F. O.; Cederbaum, L. S.; Tarantelli, F. *Phys. Rev. A* **1996**, *53*, 2118.
(36) Tarantelli, F.; Cederbaum, L. S.; Sgamellotti, A. *J. Electron Spectrosc.* **1995**, *76*, 47.
(37) Ohno, M.; Zakrzewski, V. G.; Ortiz, J. V.; von Niessen, W. *J. Chem. Phys.* **1997**, *106*, 3258.
(38) Dolgounitcheva, O.; Zakrzewski, V. G.; Ortiz, J. V. *J. Chem. Phys.* **2001**, *114*, 130.
(39) Santra, R.; Cederbaum, L. S. *Phys. Rev. Lett.* **2003**, *90*, 153401.
(40) Müller, I. B.; Zobeley, J.; Cederbaum, L. S. *J. Chem. Phys.* **2002**, *117*, 1085.
(41) Buth, C.; Santra, R.; Cederbaum, L. S. *J. Chem. Phys.* **2003**, *119*, 10575.
(42) Villani, C.; Tarantelli, F. *J. Chem. Phys.* **2004**, *120*, 1775.
(43) Meyer, H.-D.; Pal, S. *J. Chem. Phys.* **1989**, *91*, 6195.
(44) Tarantelli, F. To be submitted for publication.
(45) Tarantelli, F.; Sgamellotti, A.; Cederbaum, L. S. *J. Chem. Phys.* **1991**, *94*, 523.
(46) GAMESS-UK is a package of ab initio programs written by Guest, M. F.; van Lenthe, J. H.; Kendrick, J.; Schoffel, K.; Sherwood, P. with contributions from Amos, R. D.; Buencker, R. D.; van Dam, H. J. J.; Dupuis, M.; Handy, N. C.; Hillier, I. H.; Knowles, P. J.; Bounacic-Koutecky, V.; von Niessen, W.; Harrison, R. J.; Rendell, A. P.; Saunders, V. R.; Stone, A. J.; Tozer, D. J.; de Vries, A. H. The package is derived from the originel GAMESS code due to Dupuis, M.; Spangler, D.; Wendoloski, J. *NRCC Software Catalog*; 1980; Vol. 1, Program No. QG01 (GAMESS).
(47) Dunning, T. H., Jr. *J. Chem. Phys.* **1989**, *90*, 1007.
(48) Woon, D. E.; Dunning, T. H., Jr. To be submitted for publication.
(49) Feller, D.; Schuchardt, K. Basis sets were obtained from the Extensible Computational Chemistry Environment Basis Set Database, version 2/12/03, as developed and distributed by the Molecular Science Computing Facility, Environmental and Molecular Sciences Laboratory, which is part of the Pacific Northwest Laboratory, P.O. Box 999, Richland, WA 99352. Contact David Feller or Karen Schuchardt for further information.
(50) Dunning, T. H., Jr. *J. Chem. Phys.* **1989**, *90*, 1007.
(51) Kendall, R. A.; Dunning, T. H., Jr.; Harrison, R. J. *J. Chem. Phys.* **1992**, *96*, 6769.
(52) Feller, D. *J. Chem. Phys.* **1992**, *96*, 6104.
(53) Müller, I. B.; Cederbaum, L. S. To be submitted for publication.
(54) Santra, R.; Cederbaum, L. S. *Phys. Rev. Lett.* **2003**, *90*, 153401.